

MICROSTRUCTURAL CHARACTERIZATION OF 5-9% CHROMIUM REDUCED-ACTIVATION STEELS—R. Jayaram (University of Pittsburgh) and R. L. Klueh (Oak Ridge National Laboratory)

OBJECTIVE

The goal of this study is to characterize the microstructures of the reduced-activation ferritic steels and relate the microstructure to the mechanical properties.

SUMMARY

The microstructures of a 9Cr-2W-0.25V-0.1C (9Cr-2WV), a 9Cr-2W-0.25V-0.07Ta-0.1C (9Cr-2WVTa), a 7Cr-2W-0.25V-0.07Ta-0.1C (7Cr-2WVTa), and a 5Cr-2W-0.25V-0.07Ta-0.1C (5Cr-2WVTa) steel (all compositions are in weight percent) have been characterized by Analytical Electron Microscopy (AEM) and Atom Probe Field Ion Microscopy (APFIM). The matrix in all four reduced-activation steels was 100% martensite. In the two 9Cr steels, the stable precipitates were blocky $M_{23}C_6$ and small spherical MC. The two lower-chromium steels contained blocky M_7C_3 and small needle-shaped carbonitrides in addition to $M_{23}C_6$. AEM and APFIM analysis revealed that in the steels containing tantalum, the majority of the tantalum was in solid solution. The experimental observations were in good agreement with phases and compositions predicted by phase equilibria calculations.

PROGRESS AND STATUS

Introduction

First wall and blanket structure materials of fusion power plants are expected to become highly radioactive during service. The ferritic steels first considered for fusion applications in the United States were commercial Cr-Mo steels: 2¼Cr-1Mo (2.25 Cr-1.0Mo-0.1 C), 9Cr-1MoVNb (9 Cr-1.0Mo-0.2V-0.06Nb-0.1C) and 12Cr-1MoVW (12Cr-1.0Mo-0.25V-0.5W-0.5Ni-0.2C). Unless stated otherwise, compositions are in weight percent. Since the disposal of radioactive waste materials poses serious problems, an important consideration in the design of the first wall and blanket structure is to minimize the induced radioactive decay times of the radioisotopes that would be formed during service [1,2]. The alloying elements that result in radioisotopes with long decay times are nickel, molybdenum, nitrogen, copper and niobium.

Reduced-activation steels were developed that were variations of the conventional ferritic/martensitic steels, with molybdenum replaced by tungsten and niobium replaced by tantalum [3]. Previous studies of such steels have indicated that a 9Cr-2WV steel with a nominal composition of 9Cr-2W-0.25V-0.1C had tensile and impact toughness properties similar to the 9Cr-1MoVNb steel that it would replace [3]. The addition of tantalum to the same nominal composition (9Cr-2WVTa) resulted in a steel with superior impact properties [4]. Neutron irradiation of ferritic steels generally causes an increase in the ductile-brittle transition temperature (DBTT) and a decrease in upper shelf energy (USE) as determined in a Charpy impact test. The low DBTT of the unirradiated 9Cr-2WVTa translated into a small shift in DBTT after irradiation. The 9Cr-2WVTa steel had the smallest change in DBTT and USE ever observed for this type of steel (conventional or reduced-activation) after irradiation in a fast reactor [3].

The objective of this study is to characterize the microstructure and chemistry of the matrix and precipitates in unirradiated 5-9% Cr reduced-activation steels using a combination of Transmission Electron Microscopy (TEM) and Atom Probe Field Ion Microscopy (APFIM). It is also of interest to gain a better understanding of these steels by comparing the experimental analytical results obtained from microanalytical techniques with phase equilibria calculations based on the ThermoCalc™ software [5].

Experimental Procedure

The steels chosen for this study were the 9Cr-2WV and 9Cr-2WVTa previously examined [3], along with a 7Cr-2WVTa and a 5Cr-2WVTa steel. The nominal compositions of the steels are given in Table 1 atom percent. Atom percent is used because it is more convenient for the calculations to be discussed later. Tensile specimens were fabricated from 0.76 mm-thick sheet and normalized by austenitizing 0.5 h at 1050°C in flowing helium and cooling in rapidly flowing helium. The steels were tempered 1 h at 750°C [6]. Thin foils were prepared from the shoulders of tensile specimens and examined in a Philips CM30 transmission electron microscope (TEM) at an operating voltage of 300 kV. X-ray energy dispersive spectrometry (XEDS) was performed in a Philips EM 400 TEM equipped with a field emission gun at an operating voltage of 100 kV. Atom probe specimens of the 9Cr-2WVTa and 7Cr-2WVTa steels were fabricated using standard techniques. The analyses were performed at 60 K and a pulse fraction of 20% in the Oak Ridge National Laboratory energy-compensated atom probe [7,8].

Table 1. Bulk compositions of the steels in atomic percent (balance iron).

Alloy	Cr	Mn	V	W	Ta	C	Si	N
9Cr-2WV	9.6	0.5	0.2	0.6		0.5	0.5	0.1
9Cr-2WVTa	9.5	0.4	0.2	0.6	0.02	0.5	0.5	0.09
7Cr-2WVTa	7.5	0.4	0.3	0.6	0.01	0.5	0.4	0.05
5Cr-2WVTa	5.0	0.5	0.3	0.6	0.01	0.5	0.4	0.03

Results and Discussion

The four steels were analyzed by TEM and XEDS, and the results will be discussed in the following sections. Results on morphology, size, and number densities of the precipitates and other microstructural features of the four steels are summarized in Table 2, along with selected mechanical properties to which the microstructural changes will be related in a later section.

Table 2. Mechanical properties and quantitative TEM estimates of microstructural features.

	9Cr-2WV	9Cr-2WVTa	7Cr-2WVTa	5Cr-2WVTa
DBTT	-60°C	-88°C	-84°C	-118°C
Yield (MPa)	597	645	583	629
lath size (μm)	0.5-0.7	0.1-0.3	0.1-0.3	0.09-0.2
grain size (μm)	65	32	11	16
M ₂₃ C ₆ (blocky) N _v (m ⁻³) Diameter (nm)	1.0x10 ¹⁹ -10 ²⁰ 100-200	1.0x10 ¹⁹ -10 ²⁰ 100-200	1.0x10 ¹⁹ -10 ²⁰ 100-200	1.0x10 ¹⁸ -10 ¹⁹ 200-400
M ₇ C ₃ (faulted) N _v (m ⁻³) Diameter (nm)	n.d. ^a	n.d.	1.0x10 ¹⁹ -10 ²⁰ 100 - 300	1.0x10 ²⁰ -10 ²¹ 100 - 300
MC (spherical) N _v (m ⁻³) Diameter (nm)	1.0x10 ¹⁷ -10 ¹⁸ 40-50	1.0x10 ¹⁷ -10 ¹⁸ 20-40	n.d.	n.d.
M(CN) _{1-x} (needle) N _v (m ⁻³) Size (nm)	n.d.	n.d.	1.0 x 10 ²³ 5-30	1.0 x 10 ²¹ 5-30

^a n.d.—not detected

Microstructure of Matrix

In a previous study, optical metallography of the 9Cr-2WV and 9Cr-2WVTa steels revealed that these materials were 100% tempered martensite [9]. The microstructures of the 7Cr-2WVTa and the 5Cr-2WVTa were also 100% martensite [10]. Previous studies also revealed that the 9Cr-2WVTa steel had a finer prior austenite grain size than the 9Cr-2WV steel [9]. TEM examinations in this study revealed that the 9Cr-2WVTa steel had a well developed and finer lath structure than the 9Cr-2WV steel (Figs. 1a and 1b), which agrees with a previous study [3]. Similar fine-sized laths were found in the 7Cr-2WVTa and 5Cr-2WVTa steels (Figs. 1c and 1d). The average grain sizes and lath sizes observed in the four steels are listed in Table 2.

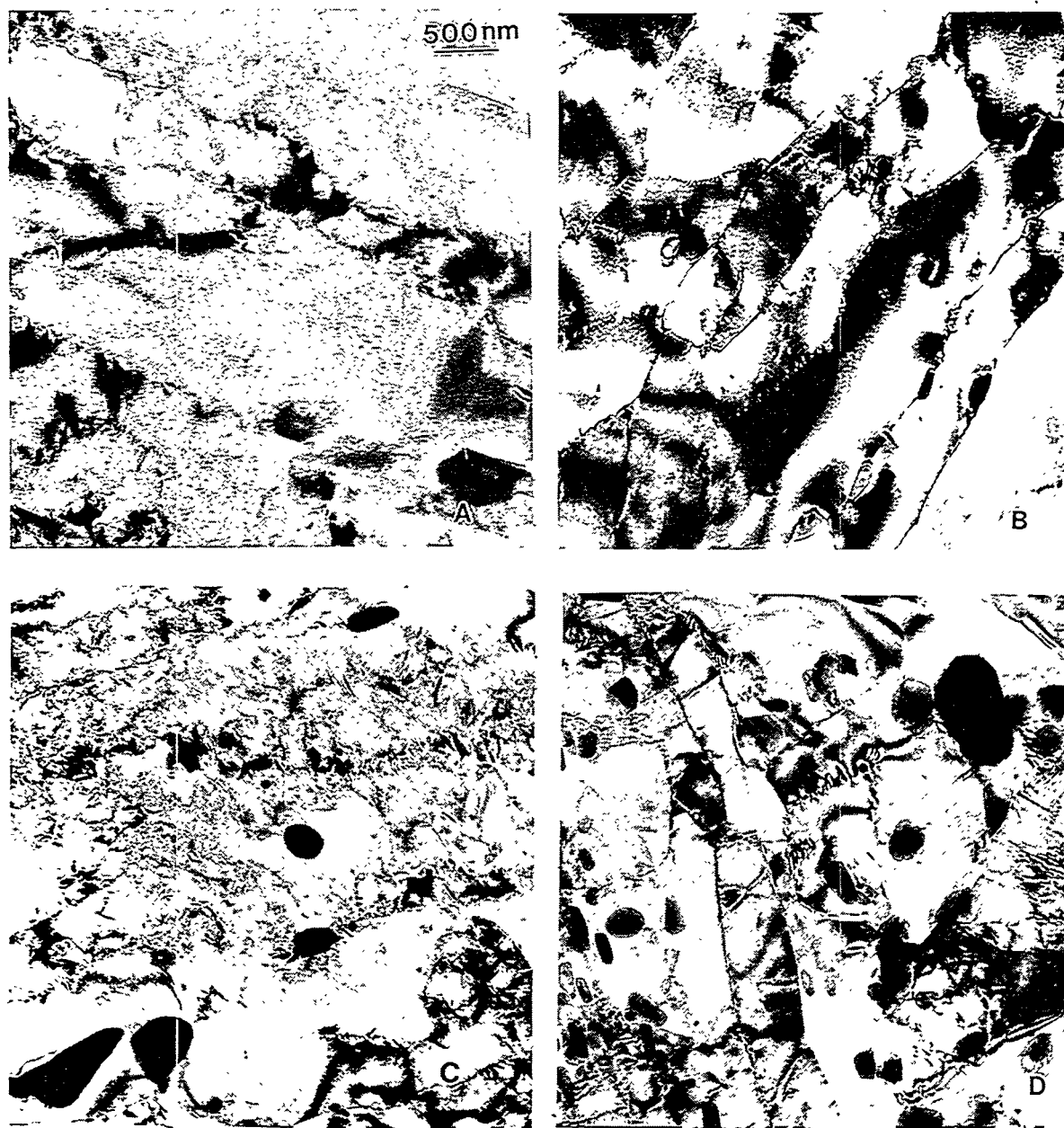


Fig. 1. Micrographs of the normalized-and-tempered (A) 9Cr-2WV, (B) 9Cr-2WVTa, (C) 7Cr-2WVTa and (D) 5Cr-2WVTa steels.

Precipitates in 9Cr-2WV

Transmission electron microscopy of the 9Cr-2WV steel revealed blocky precipitates that were identified as $M_{23}C_6$ based on selected area diffraction patterns. These precipitates displayed a cube-on-cube orientation relationship with the matrix; they were also detected at lath boundaries and prior austenite grain boundaries. Small spherical precipitates (30-50 nm in diameter) at number densities approximately two orders of magnitude lower than those of the $M_{23}C_6$ precipitates were also encountered. These precipitates have been previously observed in both 9Cr steels and have been reported to be V-rich MC precipitates in the 9Cr-2WV steel and V-rich or Ta-rich MC precipitates in the 9Cr-2WVTa steel [9]. The blocky $M_{23}C_6$ precipitates and the small spherical precipitates (arrows) are shown in Fig. 2.



Fig. 2. Transmission electron micrograph of the 9Cr-2WVTa steel showing blocky $M_{23}C_6$ and small spherical MC (arrows) precipitates.

Precipitates in 9Cr-2WVTa

The precipitates in the 9Cr-2WVTa steel were similar to those in the 9Cr-2WV steel. Blocky $M_{23}C_6$ and the small spherical precipitates previously identified as MC [9] were detected in the matrix and at lath boundaries. Precipitate sizes and number densities were comparable to those in the 9Cr-2WV steel, although the small spherical precipitates in the 9Cr-2WVTa steel, most of which were vanadium rich with a few being tantalum rich, appeared to be somewhat smaller than those in the 9Cr-2WV steel.

Precipitates in 7Cr-2WVTa

Blocky $M_{23}C_6$ precipitates were observed in the 7Cr-2WVTa with a similar size and number density range as in the two 9Cr steels (Table 2). In addition, blocky faulted M_7C_3 precipitates (Fig.3) and small needle-shaped precipitates approximately 5 nm in diameter and 30 nm long (Fig. 4) were detected in high number densities in the 7Cr-2WVTa steel. Neither the M_7C_3 nor the needle-shaped precipitates were detected in the 9Cr steels. As discussed later, the needle-shaped precipitates

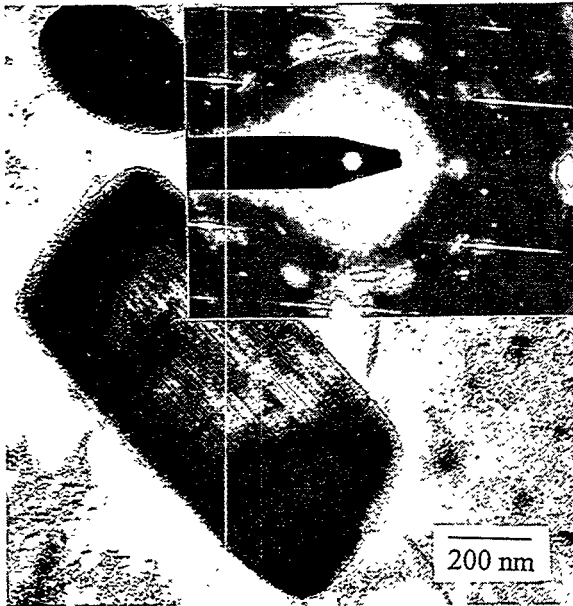


Fig. 3. Micrograph of faulted M_7C_3 precipitates in the in the 7Cr-2WVTa steel. Inset shows typical selected area diffraction pattern.



Fig. 4. Micrograph of needle-like carbonitrides in the 7Cr-2WVTa steel.

were concluded to be vanadium carbonitrides. The needle-shaped precipitates were imaged in the field ion microscope (FIM) as brightly-imaging regions approximately 2-5 nm in diameter (Fig. 5). The small spherical precipitates detected in the 9Cr steels were not detected in 7Cr-2WVTa steel.

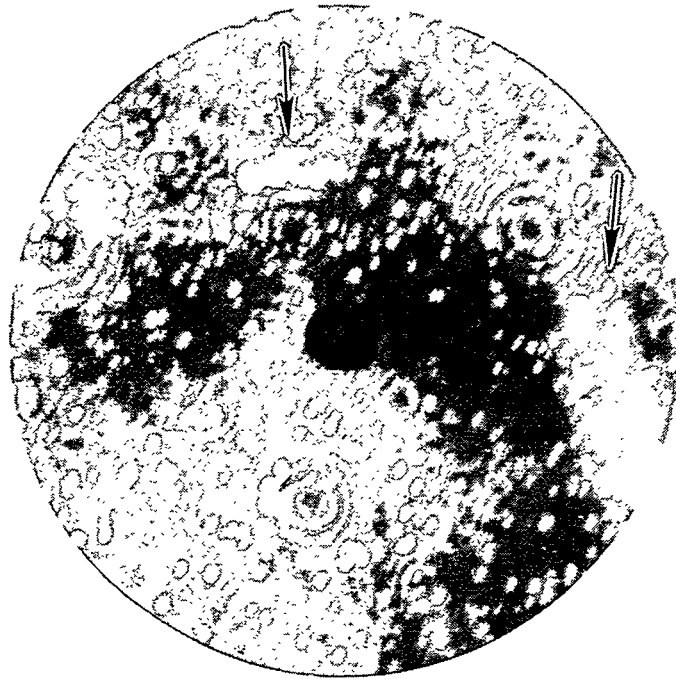


Fig. 5. Field ion micrograph of a specimen of the 7Cr-2WVTa steel showing brightly-imaging needle-like $M(CN)_{1-x}$ precipitates (arrows).

Precipitates in 5Cr-2WVTa

Precipitates in the 5Cr-2WVTa steel were $M_{23}C_6$, M_7C_3 and the needle-shaped particles. The number density of the M_7C_3 precipitates was somewhat higher than in the 7Cr-2WVTa steel, and the needle-shaped particles occurred in approximately two orders of magnitude lower number densities compared to the 7Cr-2WVTa steel. As in the 7Cr-2WVTa steel, the small spherical precipitates found in the 9Cr steels were absent (Table 2).

Microchemistry of Matrix

Atom probe analyses of the 9Cr-2WV, 9Cr-2WVTa, and 7Cr-2WVTa steels revealed that the matrix was depleted of the solutes Cr, W, V, and C. Analysis of the 9Cr-2WVTa and 7Cr-2WVTa steels indicated that a substantial portion of the tantalum was in solution, as shown in Table 3. The fragile nature of these steel specimens precluded the atom probe analysis of the large data blocks (>100,000 ions) necessary to obtain improved statistics on the matrix concentration of tantalum. However, the atom probe estimate of the matrix concentration of tantalum is consistent with the previous AEM observation on 9Cr-2WVTa [9], which indicated that tantalum is present only in the small spherical particles which occurred in low number densities.

Table 3. Atom probe analysis and ThermoCalc™ predictions of matrix composition atom percent of the 7Cr and 9Cr steels (balance iron).

Alloy		Cr	V	W	Ta	C	Si
9Cr-2WV	AP ^a	8.0 ± 0.2	0.1 ± 0.02	0.3 ± 0.03		0.01 ± 0.01	0.4 ± 0.04
	TC ^b	8.3	0.2	0.50		0.01	0.5
9Cr-2WVTa	AP	7.8 ± 0.2	0.2 ± 0.04	0.4 ± 0.04	0.02 ± 0.01	0.02 ± 0.01	0.6 ± 0.05
	TC	8.5	0.2	0.5	0.02	0.01	0.5
7Cr-2WVTa	AP	6.4 ± 0.2	0.07 ± 0.02	0.5 ± 0.06	0.02 ± 0.01	0.01 ± 0.01	0.3 ± 0.04
	TC	6.5	0.2	0.5	0.02	0.01	0.4

^a AP—Determined by the atom probe.

^b TC—Calculated with the ThermoCalc software.

Phase predictions for the compositions under discussion were made with the ThermoCalc software; detailed discussions of the calculations are given below. In Table 3, the matrix concentration of alloying elements in 9Cr-2WVTa and 7Cr-2WVTa steels determined by atom probe are compared with the predictions of ThermoCalc. There appears to be reasonably good agreement between the experimental results and ThermoCalc with regard to the 9Cr-2WV and 9Cr-2WVTa steels, although the Cr concentration, as estimated by ThermoCalc, is slightly higher than the experimental value in the two 9Cr steels. An possible explanation for the lower atom probe concentrations of Cr is that the region of analysis in the matrix was in a Cr-depleted region in close proximity to a large $M_{23}C_6$ or M_7C_3 precipitate. However, it is important to note that the trends predicted by ThermoCalc are in broad agreement with experimental results. The calculations predict that tantalum, at these concentrations, does not partition to any of the carbide phases but is present in the tempered martensite matrix. The severe depletion of carbon and to a lesser extent the depletion of W and V are also consistent with the observation of various carbide phases in these steels.

Microchemistry of Precipitates—General

A comparison of the precipitate compositions determined by XEDS and APFIM with predicted compositions obtained from phase equilibria calculations using ThermoCalc is depicted in Table 4. The

Table 4. Compositions of carbides in atomic percent (balance iron) determined by XEDS and calculated with ThermoCalc™. The XEDS compositions are normalized to the overall stoichiometry based on experimental values, which indicate only the metallic content.

Alloy		Carbide	Cr	W	Ta	V	C	N
9Cr-2WV	Expt ^a	M ₂₃ C ₆	46.7	4.6		0.9		
		MC ^b	8.3	0.5		44.2		
	TC ^c	M ₂₃ C ₆	50.4	4.8		0.0	20.7	0.0
		M(CN) _{1-x}	0.2	0.02		53.0	10.3	36.4
9Cr-2WVTa	Expt ^a	M ₂₃ C ₆	42.1	4.6				
		MC ^a	2.9	0.5	41.2	5.7		
	TC	M ₂₃ C ₆	50.6	4.8	0.0	0.02	20.7	0.0
		M(CN) _{1-x}	0.1	0.02	0.0	52.9	8.5	38.2
7Cr-2WVTa	Expt ^d	M ₂₃ C ₆	41.7	1.8				
		M ₇ C ₃	39.2	4.0		3.2		
		M(CN) _{1-x}	8.3	9.0		42.9	27.4	12.4
	TC	M ₂₃ C ₆	47.0	4.8	0.0	0.03	20.7	0.0
		M ₇ C ₃	53.4	0.5	0.0	5.5	30.0	0.0
		M(CN) _{1-x}	0.7	0.2	0.0	52.4	24.3	22.4

^aExperimental determination of M₂₃C₆ and M₇C₃ was by XEDS.

^bData taken from Ref. 13.

^cCalculated with ThermoCalc.

^dExperimental determination of M₂₃C₆ and M₇C₃ was by XEDS and M(CN)_{1-x} was by Atom Probe.

results of atom probe analyses performed on the 9Cr-2WV, 9Cr-2WVTa and 7Cr-2WVTa steels reveal that the experimentally observed phases and their compositions follow the trend predicted by ThermoCalc, with the exception of the identity of the small spherical precipitates in the 9Cr steels. This discrepancy will be discussed in a later section.

Microchemistry of Precipitates in 9Cr-2WV

The compositions of the M₂₃C₆ precipitates in the 9Cr-2WV as determined by XEDS revealed them to be chromium rich with smaller amounts of tungsten and vanadium, with the balance of the metallic component being iron (Table 4). Previous XEDS studies on carbon film replicas of 9Cr-1MoVnNb-2Ni [11] and atom probe analyzes of 12% Cr steel weld metals [12] indicated that the iron content is close to 25%. The number densities of the small spherical precipitates were not high enough to be detected in the atom probe. Carbon film replica analyses from a previous study indicated that these were MC precipitates that were vanadium rich [13].

Microchemistry of Precipitates in 9Cr-2WVTa

The composition of M₂₃C₆ precipitates in the 9Cr-2WVTa was similar to that in the 9Cr-2WV steel. Analyses of foil specimens by XEDS indicated that some of the small spherical precipitates contained tantalum. Previous analyses of carbon film replicas revealed two kinds of these MC precipitates in this steel [13]: some were rich in vanadium, similar to those in the 9Cr-2WV steel, and others were rich in tantalum. The Ta-rich precipitates contained up to 41 at. % Ta [13].

A rough calculation of the amount of tantalum in the spherical precipitates was made based on the TEM estimates of number density, mean precipitate diameter, and the tantalum content of the precipitates as determined by XEDS. It was assumed that the spherical particles had a similar structure and unit cell as TaC. The calculation revealed that approximately 2% of the total tantalum concentration in the bulk went into the precipitates. Since tantalum was not detected in any of the other precipitates, the implication is that the majority of the tantalum (98%) must remain in solid solution, consistent with the atom probe results in Table 3.

Microchemistry of Precipitates in 7Cr-2WVTa

In addition to $M_{23}C_6$, M_7C_3 precipitates were also analyzed in the 7Cr-2WVTa. Although these precipitates are also chromium rich, the Cr, W and V concentrations are higher compared to the $M_{23}C_6$ precipitates (Table 4). The small size of the needle-shaped precipitates in the 7Cr-2WVTa alloy precluded reasonable XEDS compositional measurements in thin foil specimens. However, the number densities of the needle-shaped precipitates were high enough to be detected in the FIM images, and atom probe analyses revealed these precipitates to be predominantly vanadium rich with high concentrations of carbon and nitrogen, leading to the conclusion that they are carbonitrides with the composition given in Table 4. The four steels used in this study contained 100-200 wppm N.

Phase Equilibria Calculations

Phase equilibria calculations with ThermoCalc were performed to gain a better understanding of the phases that are experimentally observed in these multicomponent alloy systems. The temperature used in the calculations was 750°C which was the temperature at which the steels were tempered. Significant carbon depletion was observed in the three steels investigated in the atom probe, and this was consistent with the TEM results, which revealed the formation of three distinct carbides in the matrix and at lath boundaries. The vanadium depletion was significantly higher in the 7Cr-2WVTa steel compared to the two 9Cr steels. This observation was consistent with the atom probe and TEM results which indicated V-rich carbonitrides $[M(CN)_{1-x}]$ precipitated in a significant number density in the 7Cr-2WVTa steel.

The ThermoCalc calculations predict that in the two 9Cr steels the most stable phases are the body-centered cubic (bcc) matrix, the $M_{23}C_6$ precipitate, and the face-centered cubic (fcc) phase, which is a predominantly V-rich carbonitride. The predicted matrix phase and its composition are in full agreement with experimental results, which revealed a 100% tempered martensite matrix depleted in Cr, W, V and C. The metallic component of the precipitates, determined by XEDS, were normalized with respect to the overall stoichiometry of the phase and appear to be in broad agreement with the values predicted by ThermoCalc. The predictions of ThermoCalc with regard to the V-rich fcc carbonitrides could not be verified experimentally because the number density of the small spherical precipitates in the 9Cr steels (observed in the TEM) were not high enough to be detected in the apex region of the APFIM specimens, and therefore, accurate elemental compositions of these small spherical precipitates could not be determined directly. However, it is likely that these precipitates are carbonitrides because XEDS measurements revealed them to be rich in vanadium, similar to those predicted by ThermoCalc [13].

The agreement between experimental results and the calculations is better for the 7Cr-2WVTa steel. ThermoCalc predicts that M_7C_3 will form in addition to $M_{23}C_6$, and the calculated compositions are in rough agreement with the experimentally determined values. The high number density of the small needle-shaped precipitates enabled their elemental compositions to be determined directly by atom probe analysis (Table 4), which revealed them to be M(CN)-type precipitates with the metallic component consisting of vanadium with some contribution from chromium and tungsten. The atom probe composition is in general agreement with the M(CN) predicted by ThermoCalc, although the concentrations of chromium and tungsten are somewhat higher than

predicted. It is possible that some matrix ions (Cr and W) were sampled by the probe hole during analysis due to the small diameter (2-5 nm) of the precipitates. The largest metallic component of the precipitates is vanadium (42.9 at. %) with nitrogen accounting for a significant portion of the non-metallic component (12.4 at. %). The direct experimental confirmation of the presence of V-rich carbonitrides in the 7Cr-2WVTa steel lends further support to the suggestion that the small spherical vanadium-rich precipitates observed in the 9Cr steels might be the carbonitrides predicted by ThermoCalc and not MC precipitates, as often referred to in the literature.

The fact that these precipitates contain nitrogen is not unexpected for two reasons. First, accurate quantitative estimates of carbon and nitrogen by XEDS are difficult to obtain and require the use of a light element detector. Secondly, it is known that nitrogen can dissolve in carbides. Honeycomb states [14]: "...there are a few elements which enter predominantly the carbide phase. Nitrogen is the most important element, and it forms carbonitrides with iron and many alloying elements." Microalloyed steels containing stable carbide and nitride formers such as vanadium and niobium are known to form carbonitrides, often designated as V(C,N), Nb(C,N), or (V,Nb)(C,N)[15]. When Tupholme et al. [16] examined a series of 9Cr-WVTa and 12Cr-WVTa reduced-activation steels with 0.75 and 3% W, 0.25-0.4% V, 0.1% Ta, 0.1% C, and 100-400 wppm N, they found small spheroidal intragranular precipitates with a cubic structure in addition to $M_{23}C_6$. The small precipitates contained tantalum and vanadium, and the authors concluded were probably carbonitrides, which they designated (V,Ta)(C,N) [16].

An interesting aspect of the phase equilibrium calculations was that ThermoCalc does not predict the fcc phase if nitrogen is totally removed as a component in the thermodynamic system in the two 9Cr steels and the 7Cr-2WVTa steel. However, when nitrogen is included in amounts as small as 20 appm, the fcc phase appears as a V-rich carbonitride containing significant amounts of nitrogen (20-30 at. %). Moreover, if nitrogen is totally absent as a component and the carbon concentration is increased above the levels in these steels (0.5 at. %), ThermoCalc predicts that the MC phase will still not form. Instead, in the 9Cr steels, the M_7C_3 phase will begin to form, in addition to $M_{23}C_6$ phase. Increasing the carbon level of the 7Cr steel merely increases the molar fraction of the M_7C_3 phase. ThermoCalc rules out the possibility of an MC phase in which carbon is the only non-metallic species for the steel compositions used in this work.

The phase equilibria calculations applied to the steels in this work clearly reveal the important role of the trace impurity nitrogen. The formation of the stable carbonitrides has implications for mechanical properties, not only in the steels in this study, but also in the much broader context of various other types of steels which contain V, Ti or Nb, all of which are known to be potent carbonitride formers.

The formation of the various phases in the 9Cr-2WV, 9Cr-2WVTa, 7Cr-2WVTa and 5Cr-2WVTa steels is related to the interplay of the relative levels of Cr, V, C and N. In the two 9Cr steels and the 7Cr-2WVTa steel, it is reasonable to assume that the addition of trace quantities of nitrogen stabilizes the fcc phase sufficiently to allow for the formation of $M(CN)_{1-x}$ along with the $M_{23}C_6$ phase. After tempering at 750°C when the chromium level is reduced to 7.5 at. %, ThermoCalc predicts that M_7C_3 begins to form as a stable phase in addition to the bcc matrix, $M_{23}C_6$, and the fcc carbonitride phases, which agrees with the observations.

At chromium levels of 5 at. %, the phase field is unchanged from that of the 7Cr-2WVTa system and the stable phases predicted by ThermoCalc are the bcc matrix, the $M_{23}C_6$ and M_7C_3 carbides, and the fcc V-rich $M(CN)_{1-x}$. All four phases were observed in TEM in the 5Cr-2WVTa steel. The number density of the M_7C_3 was higher and that of the needle-shaped precipitates lower than in the 7Cr-2WVTa steel (Table 2). The number density of the $M_{23}C_6$ precipitates was also somewhat lower than in the 7Cr-2WVTa steel. An interesting aspect of the phase equilibria calculations in this steel is that ThermoCalc predicts the formation of the fcc V-rich carbide in the absence of nitrogen. Although an atom probe analysis was not performed on the 5Cr-2WVTa steel to confirm this

prediction, ThermoCalc results revealed that with 300 appm N present in the bulk, the fcc phase has the composition 47.2 at. % V-2.9% Cr-3.3% W-0.1% Fe-40.9% C-5.6% N. This result indicates that even with nitrogen present in the alloy the fcc precipitate is predominantly carbon rich with a nitrogen concentration of only 5%.

Mechanical Properties

Since mechanical properties are influenced by microstructural features, it is important to consider how the microstructures of the four steels relate to the mechanical properties. A comparison of the Charpy impact properties of the 9Cr-2WV and 9Cr-2WVTa steel revealed significant differences (Table 2). The DBTT of the 9Cr-2WV and 9Cr-2WVTa in the normalized-and-tempered condition was -60 and -88 °C, respectively, while the USE was 8.4 and 11.2 J, respectively [3]. These results were taken to indicate the effect of tantalum on the properties [3].

A significant difference between the microstructure of the 9Cr-2WVTa steel and the 9Cr-2WV steel was in the finer prior austenite grain size [10] and smaller lath size of the steel containing tantalum. Although atom probe analysis revealed that the majority of the tantalum is in solid solution in the Ta-containing alloys, some small fraction could conceivably segregate to grain and lath boundaries and thereby provide a mechanism for grain refinement. Further experimental work is needed to verify this suggestion. Previous work concluded that tantalum in solution has a significant effect on the Charpy properties of the 9Cr-2WVTa steel relative to the 9Cr-2WV steel, perhaps by increasing the fracture stress of the 9Cr-2WVTa [17]. The atom probe results that indicate that most of the tantalum remains in solution reinforces that conclusion.

It has been suggested in the literature that better fracture toughness correlates with lower Cr content in a steel [18]. Superficially, this suggestion seems to be supported by experimental data for the reduced-activation steels of this study (Table 4) and previous studies [4,10]. The USE of a 9Cr-2WV and a 5Cr-2WV steels were 9.5 and 11.7 J, respectively [4]; the USE of the 9Cr-2WVTa, 7Cr-2WVTa and 5Cr-2WVTa steels were 10.1, 11.4, and 14.3 J, respectively [10]. Likewise, although the 9Cr-2WVTa and 7Cr-2WVTa steels have similar DBTTs, the DBTT for 5Cr-2WVTa is considerably lower than those of the other steels (Table 2), again indicating the possible effect of chromium. As pointed out above, tantalum affects the DBTT [3,4], but its effect on the USE is not as obvious.

The size and number density of the $M_{23}C_6$ precipitates were nearly the same in all four steels, and $M_{23}C_6$ probably does not influence the differences in the mechanical behavior of these steels. Similar arguments apply to the large M_7C_3 precipitates in the 7Cr-2WVTa and 5Cr-2WVTa steels. The small $M(CN)_{1-x}$ precipitates might be expected to contribute to an increase in the yield stress through precipitate hardening in the 7Cr-2WVTa steel, where they occur in significant number densities. This argument is not, however, borne out by yield stress data (Table 2). The room temperature yield stress of the 7Cr-2WVTa steel was 583 MPa compared to 645 MPa for the 9Cr-2WVTa, 629 MPa for the 5Cr-2WVTa, and 597 MPa for the 9Cr-2WV steels [10], thus giving no indication of a discernible trend, even though the Charpy properties appear to be sensitive to the microstructural differences.

SUMMARY AND CONCLUSIONS

The microanalytical characterization of four reduced activation 5-9% Cr steels revealed that the matrix was 100% tempered martensite. Blocky (100-200 nm) Cr-rich $M_{23}C_6$ formed in all four steels. The 9Cr-2WV and 9Cr-2WVTa steels also contained small spherical V-rich and V- or Ta-rich precipitates, respectively. Analysis of the 7Cr-2WVTa and 5Cr-2WVTa alloys revealed Cr-rich blocky faulted M_7C_3 in the matrix and at lath boundaries. Small V-rich needle-shaped $M(CN)_{1-x}$ in high number densities were also detected in the 7Cr-2WVTa and 5Cr-2WVTa steels. The XEDS and atom probe analysis revealed that with the exception of a few of the small spherical precipitates, no tantalum was detected in any of the other precipitates. Atom probe analysis of the matrix

indicated a depletion of Cr, W, V, and C and that nearly all the tantalum was in solid solution in the tantalum-containing steels.

The experimentally observed stable phases and their compositions are in general agreement with phase equilibria calculations using the ThermoCalc software. The thermodynamic calculations revealed the important role of trace amounts of nitrogen in these alloys. ThermoCalc predicts the absence of the V-rich fcc carbide as a stable phase in the 9Cr-2WVTa and 7Cr-2WVTa steels unless nitrogen is present in the system as a trace impurity in quantities as low as 20 appm. Atom probe analysis of the needle-shaped precipitates in the 7Cr-2WVTa steel directly confirmed the presence of these carbonitrides and revealed that these precipitates contained significant levels of nitrogen (12 at. %). These results support the argument that the small spherical precipitates in the 9Cr-2WV and 9Cr-2WVTa steels are also V-rich carbonitrides and not MC.

REFERENCES

1. R.L. Klueh and E.E. Bloom, *Nucl. Eng. Design/Fusion*, 1985, vol. 2, pp. 383-89.
2. R.W. Honeycombe, *Structure and Strength of Alloy Steels*, Climax Molybdenum Company, London 1974.
3. R.L. Klueh, *JOM*, 1992, vol. 44, p. 20-24.
4. R.L. Klueh, D.J. Alexander and P.J. Maziasz, *J. Nucl. Mater.*, 1992, vol. 186, p. 185-195.
5. B. Sundman, B. Jansson and J.O Andersson, *Calphad*, vol. 9, 1985, 153.
6. R.L. Klueh and P.J. Maziasz, *Reduced Activation Materials for Fusion Reactors*, ASTM STP 1047, edited by R.L. Klueh, D.S. Gelles, M. Okada and N.H. Packan, American Society for Testing and Materials, Philadelphia, 1990, pp.140.
7. M.K. Miller and G.D.W. Smith, *Atom Probe Microanalysis: Principles and Applications to Materials Problems*, Materials Research Society, Pittsburgh, PA, 1989.
8. M.K. Miller, *J. de Physique*, vol. 47-C2, 1986, pp. 493.
9. R.L. Klueh and P.J. Maziasz, *Metall. Trans. A*, vol. 20A, 1989, pp. 373-382.
10. R.L. Klueh, Oak Ridge National Laboratory, unpublished research, 1995.
11. P.J. Maziasz and R.L. Klueh, *Effects of Radiation on Materials: 14th International Symposium*, vol. 1, ASTM, STP 1046, edited by N.H. Packan, R.E. Stoller and A.S. Kumar, American Society for Testing Materials, Philadelphia, 1989, pp.35.
12. G. J. Cai, L. Lundin, H. O. Andrén and L. E. Svensson, *App.Surf. Sci.*, vol. 76/77, 1994, pp. 248.
13. R.L. Klueh, P.J. Maziasz and W.R. Corwin, *Development of Ferritic Steels for Fusion Reactor Applications*, Report No.6472, ORNL, 1988.
14. R. W. K. Honeycomb, *Steels: Microstructure and Properties*, Edward Arnold, London, 1981, pp. 61.
15. M. J. Crooks, A. J. Garratt-Reed, J. B. Vander Sande, and W. S. Owen, *Met. Trans. A.*, vol. 12A, 1981, pp. 1999.
16. K. W. Tupholme, D. Dulieu, and G. J. Butterworth, *J. Nucl. Mater.*, vol. 179-181, 1991, pp.684.
17. R.L. Klueh, D.J. Alexander and P.J. Maziasz, *J. Nucl. Mater.*, 1996, vol. 233-237, pp. 336.
18. H. O. Andrén, G. Cai and L. E. Svensson, *App. Surf. Sci.*, vol. 87/88, 1995, pp. 200.